

Supplementary material for Genau et al.

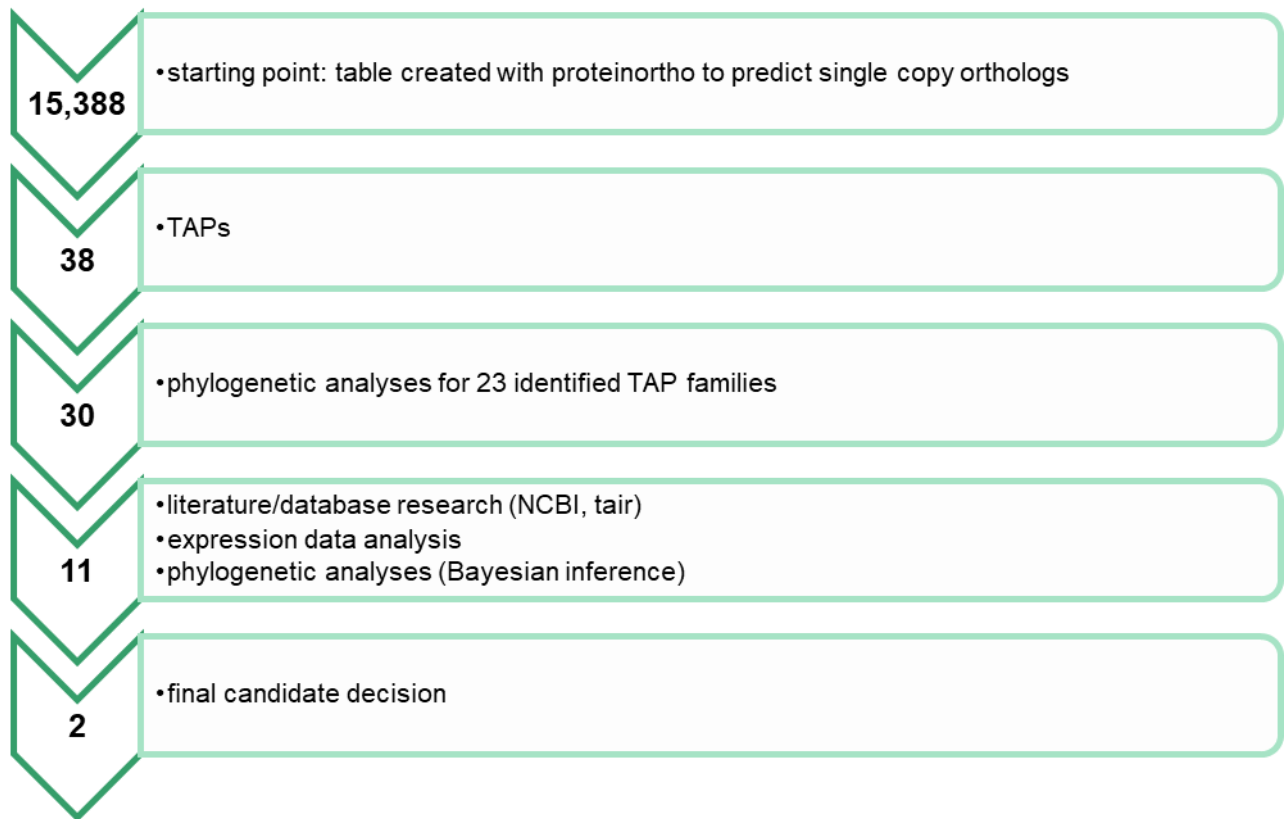


Figure S1: Workflow of phylogenetic singly copy TF/TR screening.

Based on a proteinortho [1] run 15,388 *P. patens*, 12,478 *M. polymorpha* and 14755 *A. thaliana* orthologous groups were filtered according to single copy status in each species. These proteins were scanned further using TAPscan [2], yielding 38 proteins classified into 23 TAP (TF or TR) families (GNAT, MYB-related, SET/Sigma70-like, FHA, PcG_MSI, Jumonji_Other, IWS1, C3H, C2H2, bHLH, TANGO2, tify, TUB, WRKY, MADS, Med7, O-FucT, BES1, CCAAT_HAP3, GRAS, HMG, ARID and Med6). For these 23 families, phylogenetic inference using Neighbour-Joining with quicktree-SD [3] was performed using the proteins of *Arabidopsis thaliana*, *Anthoceros agrestis*, *Marchantia polymorpha*, *Physcomitrium patens* as well as *Oryza sativa* to verify single copy status in the three bryophytes of interest, leading to removal of 8 genes on account of unclear/lack of orthology. For the remaining 30 proteins initial literature and expression analyses were conducted, narrowing them down to 11 candidates (Table S1) from which 2 were selected for this study.

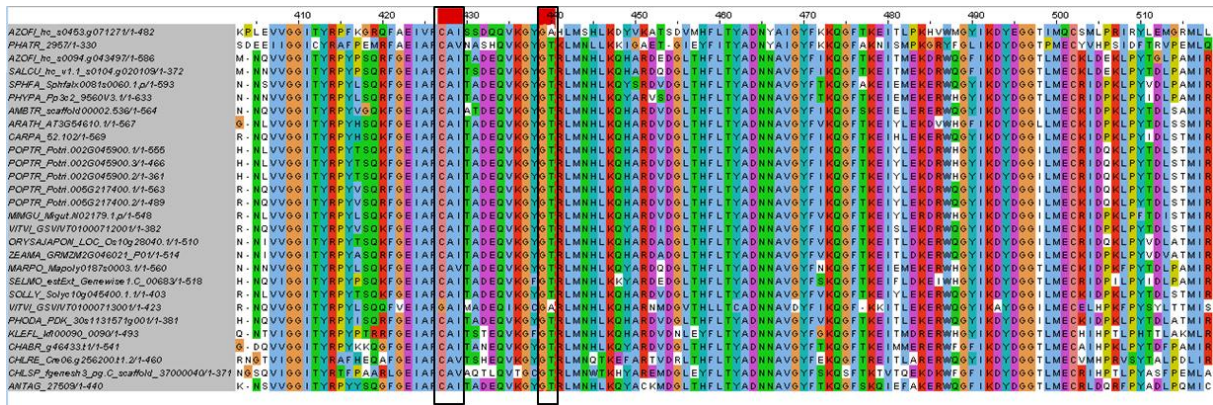


Figure S2: Multiple sequence alignment of the GNAT domain of HAG1.

The conserved Coenzyme A binding pocket is marked by black boxes.

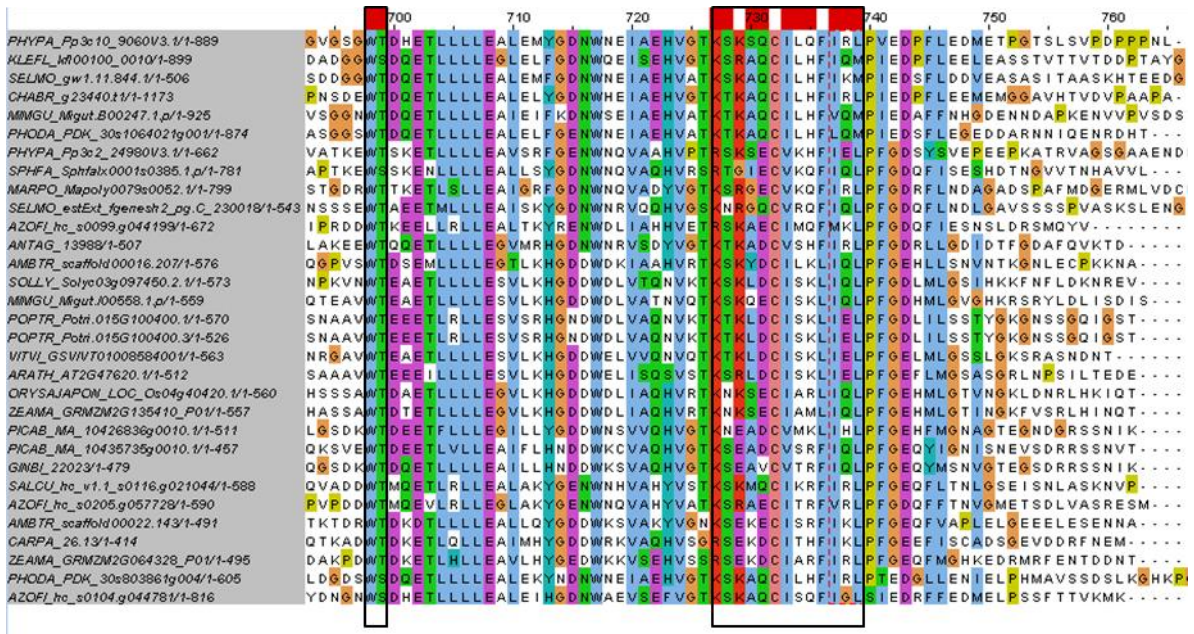


Figure S3: Multiple sequence alignment of part of the SANT/MYB domain of SWI3A/B.

The potential DNA binding sites of the MYB domain are marked by black boxes.

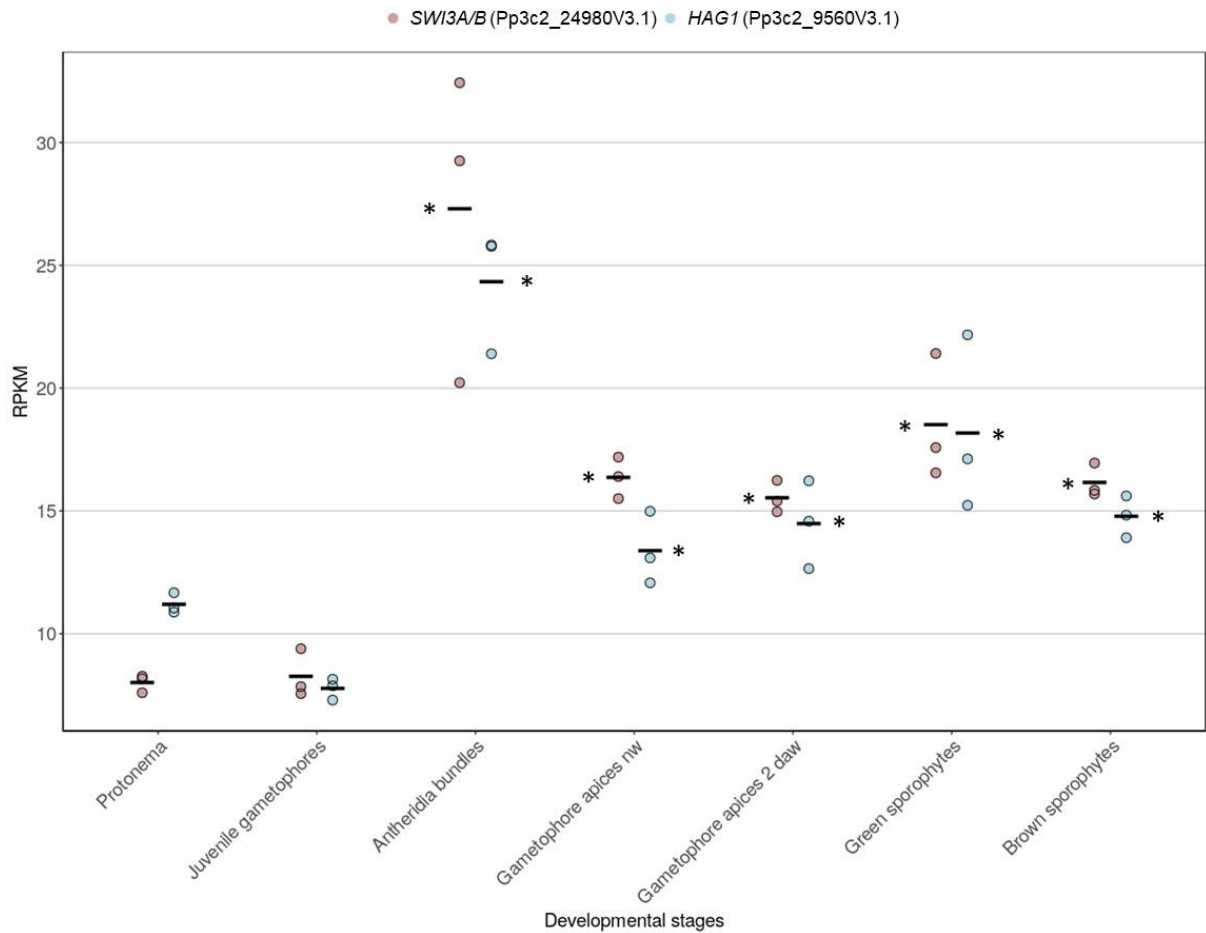


Figure S4: RNA-seq expression profile of *PpHAG1* (Pp3c2_9560V3.1, histone acetyltransferase) and *PpSWI3A/B* (Pp3c2_24980V3.1, chromatin remodelling complex subunit).

Data are from [4], antheridia bundles from [5] and apices from this study. The highest expression of both genes can be detected in antheridia bundles, but expression in all reproductive stages shown is significantly (t-test, $p < 0.05$; asterisks) higher than in the vegetative control (protonema and juvenile = asexual gametophores). Expression data in archegonia, representing the female germ line [6] is not significantly higher than in vegetative tissue (data not shown because from microarray / different scale). Gametophore apices feature gametangia (female archegonia and male antheridia). Green sporophytes are pre-meiotic, brown sporophytes post-meiotic. RPKM is Reads Per Kbp (of transcript) and Million (of reads); data were generated according to standardized procedures allowing to compare across samples [7].

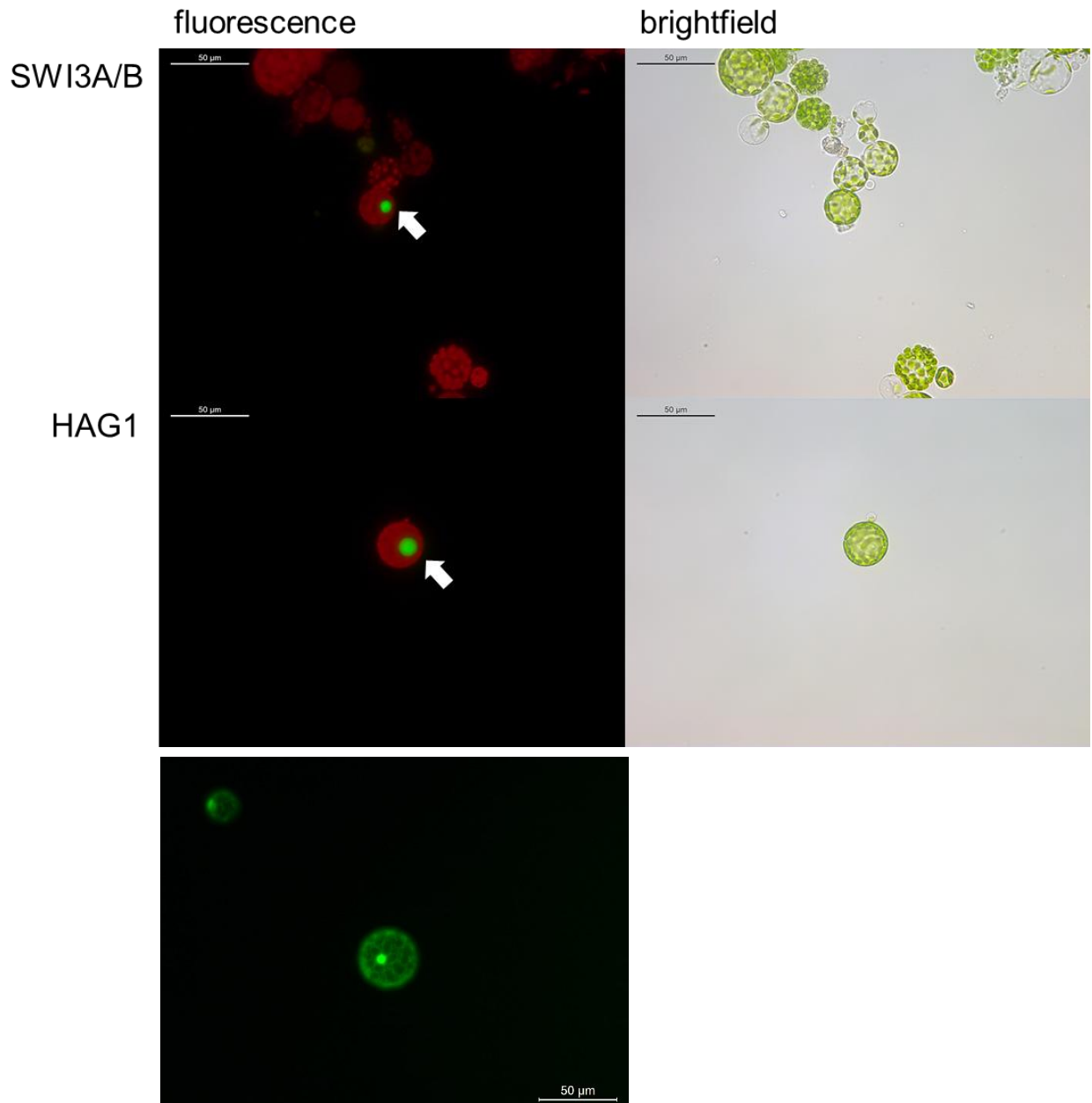


Figure S5: *In vivo* localization analysis.

Transient expression of PpSWI3A/B and PpHAG1 fused to a C-terminal GFP. The white arrows indicate the nuclear localization. A protoplast transiently expressing GFP in the nucleo-/cytoplasm is shown for comparison.

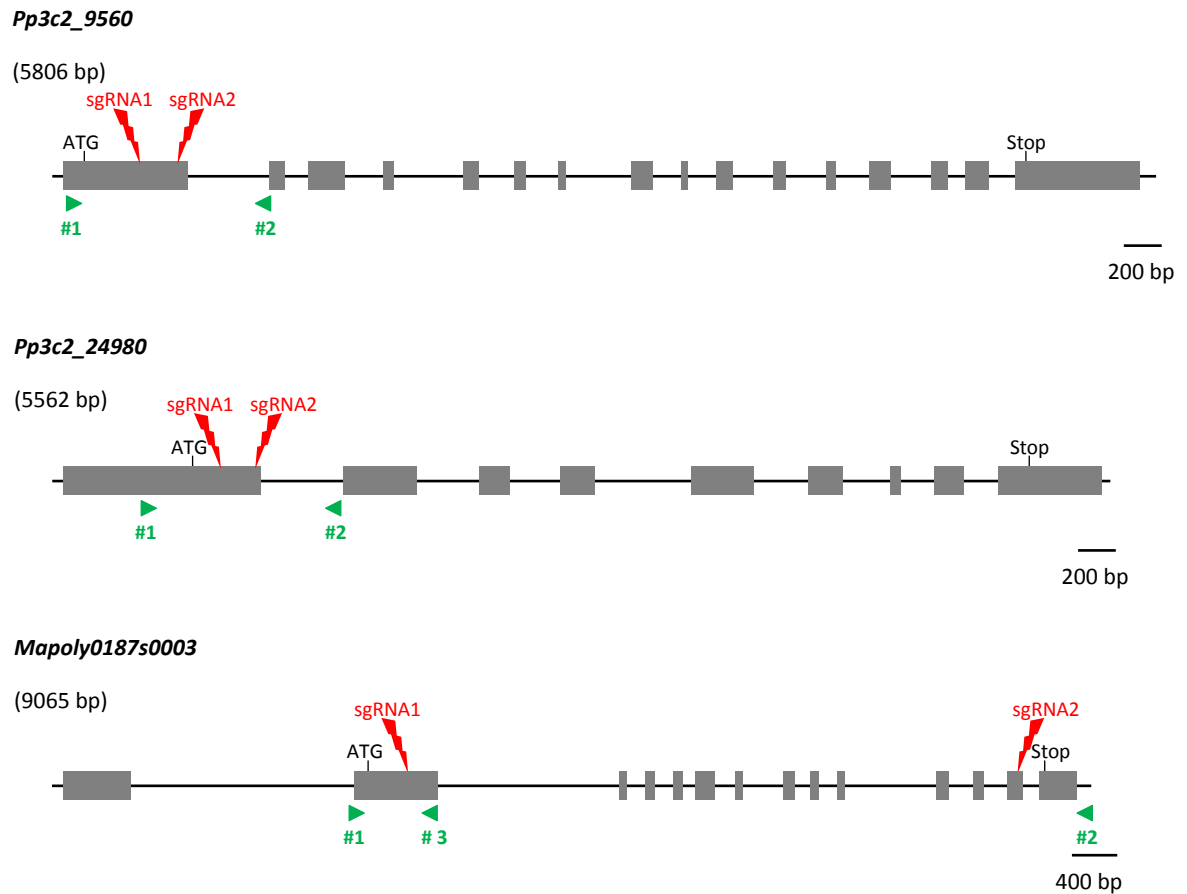


Figure S6: Structure of the *Pp3c2_9560*, *Pp3c2_24980* and *Mapoly0187s0003* targeted genes.

Structure of the *Pp3c2_9560*, *Pp3c2_24980* and *Mapoly0187s0003* genes with their respective sgRNAs positions. Boxes represent the exons and black lines represent the introns. The two sgRNAs positions are indicated (in red). Green arrows represent the primers used for PCR and sequencing.

901 915

Wild-Type ATGGAGTTGCATAGT
Swi3a/b-1 ATGGAGTTGCATAGT
Swi3a/b-2 ATGGAGTTGCATAGT
Swi3a/b-3 ATGGAGTTGCATAGT

B

1 100
Wild-Type TCCAACGGTGATTCTCGCAGCGTAAGAATCAATCACTGCTCTAGATTGAAATGGTGGCAGAGATGGCGTCACAGCAGTTCTCGGTGACGCTGTGCCATC
hag1-1 TCCAACGGTGATTCTCGCAGCGTAAGAATCAATCACTGCTCTAGATTGAAATGGTGGCAGAGATGGCGTCACAGCAGTTCTCGGTGACGCTGTGCCATC
hag1-2 TCCAACGGTGATTCTCGCAGCGTAAGAATCAATCACTGCTCTAGATTGAAATGGTGGCAGAGATGGCGTCACAGCAGTTCTCGGTGACGCTGTGCCATC
hag1-3 TCCAACGGTGATTCTCGCAGCGTAAGAATCAATCACTGCTCTAGATTGAAATGGTGGCAGAGATGGCGTCACAGCAGTTCTCGGTGACGCTGTGCCATC

101 200
Wild-Type GCCATCGCCATCGCCGTCGTATTTCGTCATTAAGCGGGTCCAGTCAGAAACGGAAACGATCCGCGCAGGATGCTGCTGCAACGGCAGACGAGTTTGTGGCA
hag1-1 GCCATCGCCATCGCCGTCGTATTTCGTCATTAAGCGGGTCCAGTCAGAAACGGAAACGATCCGCGCAGGATGCTGCTGCAACGGCAGACGAGTTTGTGGCA
hag1-2 GCCATCGCCATCGCCGTCGTATTTCGTCATTAAGCGGGTCCAGTCAGAAACGGAAACGATCCGCGCAGGATGCTGCTGCAACGGCAGACGAGTTTGTGGCA
hag1-3 GCCATCGCCATCGCCGTCGTATTTCGTCATTAAGCGGGTCCAGTCAGAAACGGAAACGATCCGCGCAGGATGCTGCTGCAACGGCAGACGAGTTTGTGGCA

201 300
Wild-Type AACTCCCCGAACCCCTTCCCTCCAACCACTCCAACGCTCACATCAAAGCGTCCACCAATCTTCTCAC.....
hag1-1 AACTCCCCGAACCCCTTCCCTCCAACCACTCCAACGCTCACATCAAAGCGTCCACCAATCTTCTCAC.....
hag1-2 AACTCCCCGAACCCCTTCCCTCCAACCACTCCAACGCTCACATCAAAGCGTCCACCAATCTAAACCTAAACCTAAACCTAAAC.....
hag1-3 AACTCCCCGAACCCCTTCCCTCCAACCACTCCAACGCTCACATCAAAGCGTCCACCAATCTTCTCAATC.....

301 400
Wild-Type AGCAGCATCCGATTATAATGCCGTTGTCTCGTGGACTCGCAGCACAGCTGCCGGAATAACCCGGGAGCTCGCTGGAGGATGAGGACGATGGGGAAAA
hag1-1
hag1-2
hag1-3

401 500
Wild-Type TGGAGGGCATCATCAGTCATGTCTCCGATGGGGTCAAGAATGGGCTAGCTATGGTTCGGTTCGAAGGTGCGAACGGCGGTGGGGATGGGGATGAAGAG
hag1-1GTGGGATGGGGATGAAGAG
hag1-2CGGCGGTGGGGATGGGGATGAAGAG
hag1-3CGGCGGTGGGGATGGGGATGAAGAG

501 600
Wild-Type GAGGACGACGATGAGGAGGAAGGCGAAGCGAAGAAAGAAAGGAGAGCACGACGAAAGGTAACCCCTAAACCTTGGTATGCCTTCGCAATCAGCGTTCT
hag1-1 GAGGACGACGATGAGGAGGAAGGCGAAGCGAAGAAAGAAAGGAGAGCACGACGAAAGGTAACCCCTAAACCTTGGTATGCCTTCGCAATCAGCGTTCT
hag1-2 GAGGACGACGATGAGGAGGAAGGCGAAGCGAAGAAAGAAAGGAGAGCACGACGAAAGGTAACCCCTAAACCTTGGTATGCCTTCGCAATCAGCGTTCT
hag1-3 GAGGACGACGATGAGGAGGAAGGCGAAGCGAAGAAAGAAAGGAGAGCACGACGAAAGGTAACCCCTAAACCTTGGTATGCCTTCGCAATCAGCGTTCT

601 700
Wild-Type TGCTCAGGCATTGGAACGGATCCTGACGATTGTGATCTGTTGTCTTATCTTCTTCTTCTTATTTTATTTTAAAGCCTACTTTGCAACTTGAAGA
hag1-1 TGCTCAGGCATTGGAACGGATCCTGACGATTGTGATCTGTTGTCTTATCTTCTTCTTCTTATTTTATTTTAAAGCCTACTTTGCAACTTGAAGA
hag1-2 TGCTCAGGCATTGGAACGGATCCTGACGATTGTGATCTGTTGTCTTATCTTCTTCTTCTTATTTTATTTTAAAGCCTACTTTGCAACTTGAAGA
hag1-3 TGCTCAGGCATTGGAACGGATCCTGACGATTGTGATCTGTTGTCTTATCTTCTTCTTCTTATTTTATTTTAAAGCCTACTTTGCAACTTGAAGA

701 800
Wild-Type CTATGCAGGAGCTTTAGCAGAGGGCTGTTTGAATGTTGGATAATGATCTTGCTTGTTTTAACTTTTAAAGATGACGGTAGTGTGGCACAATGATCGT
hag1-1 CTATGCAGGAGCTTTAGCAGAGGGCTGTTTGAATGTTGGATAATGATCTTGCTTGTTTTAACTTTTAAAGATGACGGTAGTGTGGCACAATGATCGT
hag1-2 CTATGCAGGAGCTTTAGCAGAGGGCTGTTTGAATGTTGGATAATGATCTTGCTTGTTTTAACTTTTAAAGATGACGGTAGTGTGGCACAATGATCGT
hag1-3 CTATGCAGGAGCTTTAGCAGAGGGCTGTTTGAATGTTGGATAATGATCTTGCTTGTTTTAACTTTTAAAGATGACGGTAGTGTGGCACAATGATCGT

```

Wild-Type  ATCTTTTATTTTTGTTTTTTTACGGCTGCCTTAATTTGTGGAACTGACTGAGAATGTGATCGTATCTCGGGAGCACCT
hag1-1    ATCTTTTATTTTTGTTTTTTTACGGCTGCCTTAATTTGTGGAACTGACTGAGAATGTGATCGTATCTCGGGAGCACCT
hag1-2    ATCTTTTATTTTTGTTTTTTTACGGCTGCCTTAATTTGTGGAACTGACTGAGAATGTGATCGTATCTCGGGAGCACCT
hag1-3    ATCTTTTATTTTTGTTTTTTTACGGCTGCCTTAATTTGTGGAACTGACTGAGAATGTGATCGTATCTCGGGAGCACCT

```

Figure S7: Sequence alignment of the targeted regions in the *HAG1* and *SWI3A/B* genes in the wild-type and respective mutants.

Alignment of (A) *SWI3A/B* and *swi3a/b-1*, *swi3a/b-2* and *swi3a/b-3* CRISPR-Cas targeted region, and (B) *HAG1* and *hag1-1*, *hag1-2* and *hag1-3* CRISPR-Cas targeted region. *SWI3A/B* (Pp3c2_24980); *HAG1* (Pp3c2_9560). Sequences of the sgRNAs used in this study to produce the mutants are in green (PAMs in bold). Substitutions, deletions, or insertions are indicated in red. Primers used to amplify and sequence the *HAG1* or *SWI3A/B* regions are in blue.

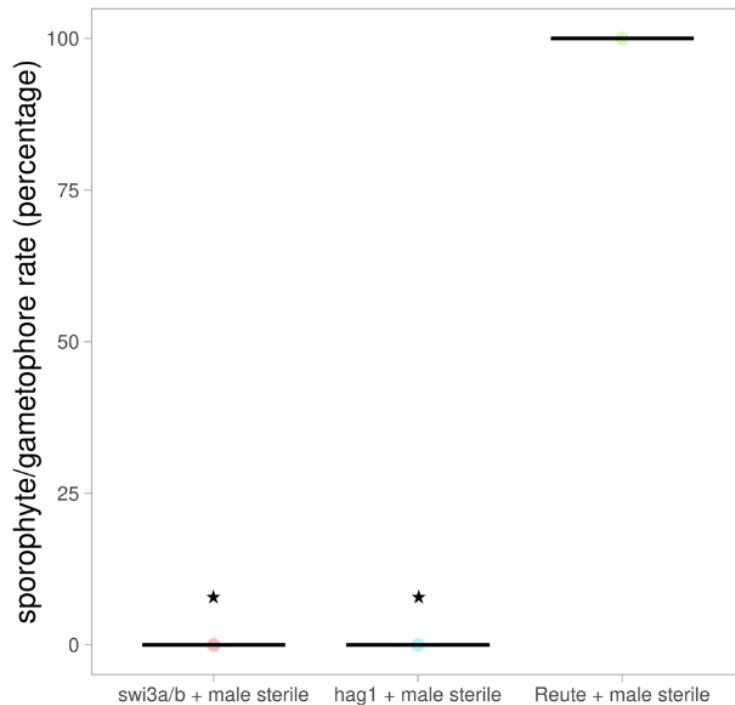


Figure S8: Crossing with a male infertile strain to test for male impairment.

Pphag1 (blue), *Ppswi3a/b* (red) and the control (Reute, green) were crossed with a male infertile strain [5]. Reute developed 100% of sporophytes per gametophore (through selfing), whereas *Ppswi3a/b* and *Pphag1* developed no sporophytes, which is a significant reduction (asterisks) ($p < 0,01$, Fisher's exact test). The total number of gametophores analysed per mutant/control was 73 each. The dots indicate the rate of sporophytes per gametophore as percentage relative to the total number of gametophores.

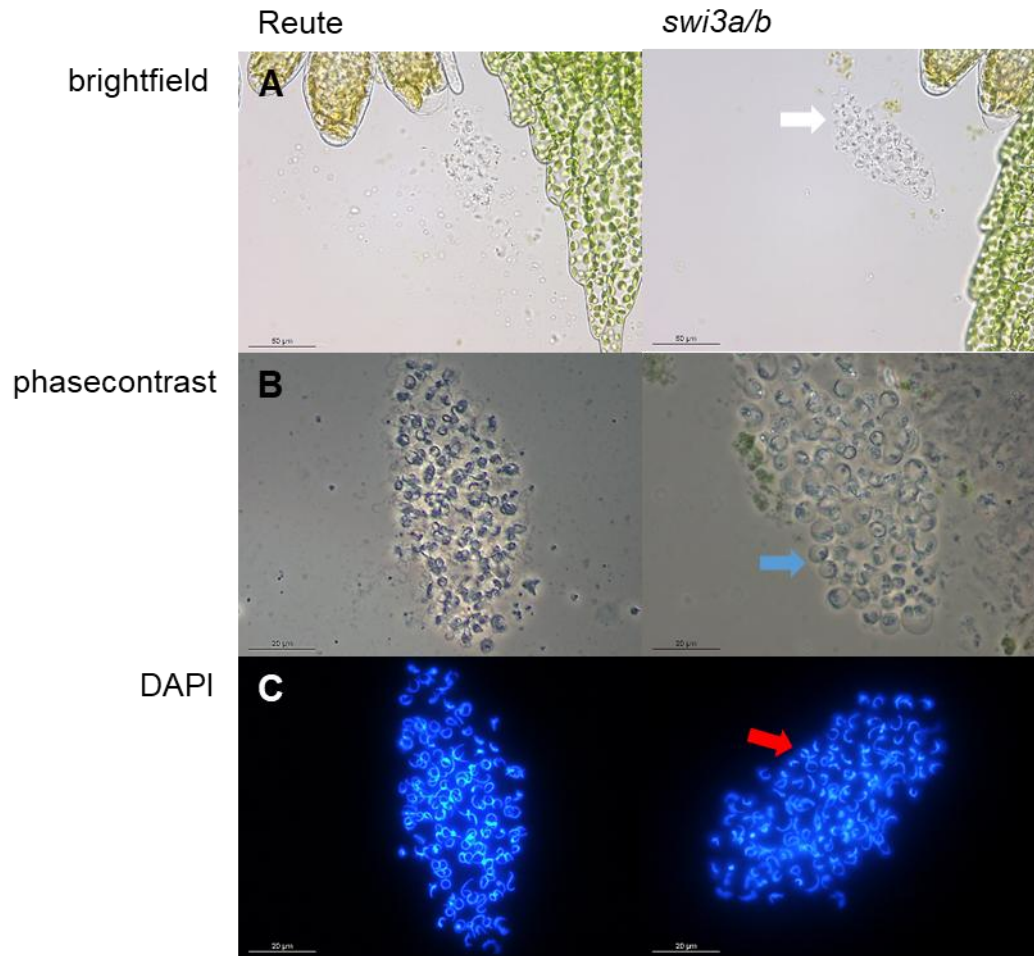


Figure S9: Spermatozoid analysis of Ppswi3a/b 21 dpi.

A) While spermatozooids of Reute as control start to move and swim shortly after release, *swi3a/b* spermatozooids are unable to swim and stick together without moving away from the antheridial bundle (indicated by white arrow). B) Phase contrast images of Reute and Ppswi3a/b. The spermatozooids of *swi3a/b* show caviar-like structures (indicated by blue arrow); cf. Figs. 6/S11. C) The DAPI staining shows fully condensed nuclei in Reute, whereas Ppswi3a/b nuclei show slight structural abnormalities / show (indicated by red arrow, cf. Fig. 6).

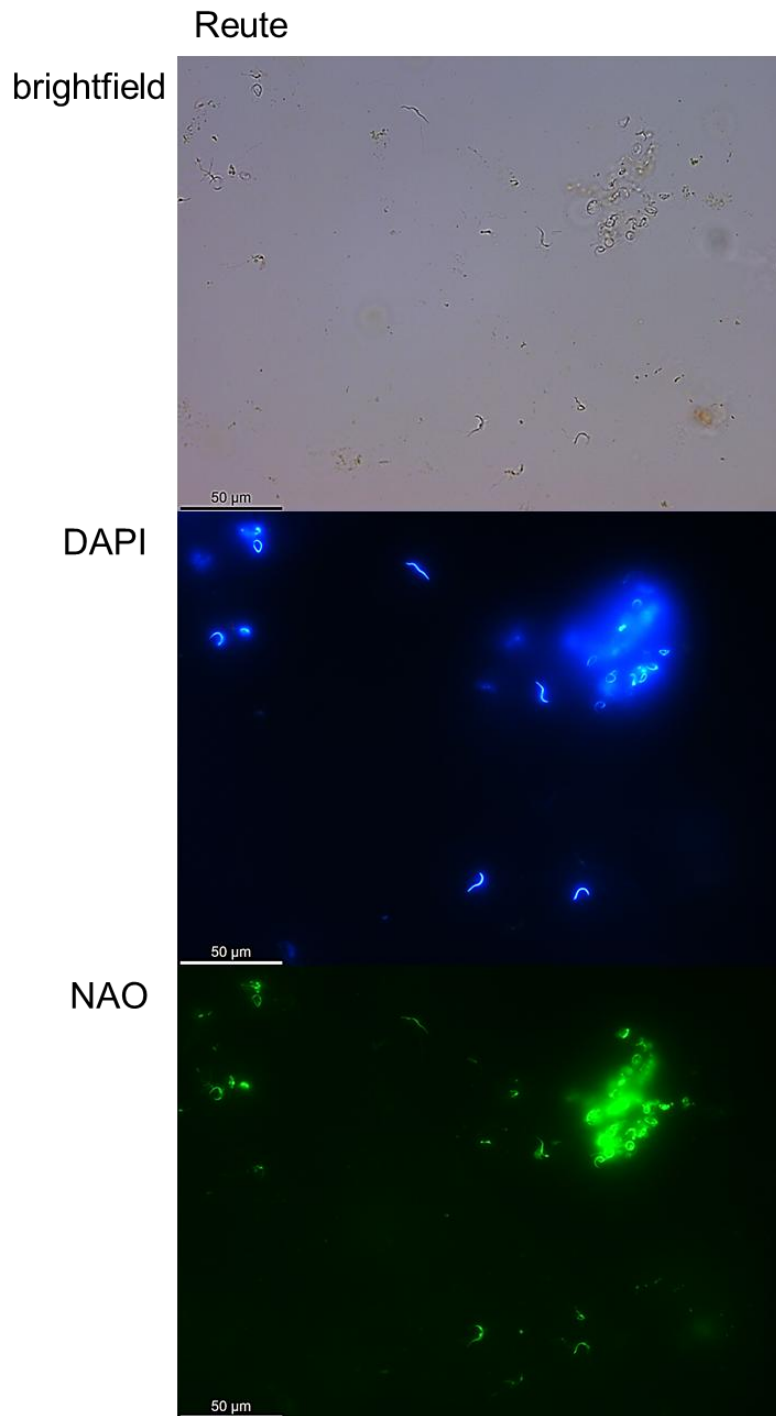


Figure S10: Spermatozoid analysis via a double staining with DAPI and NAO.

Several released Reute (control) spermatozooids are shown with their slender shape and fully reduced cytoplasm.

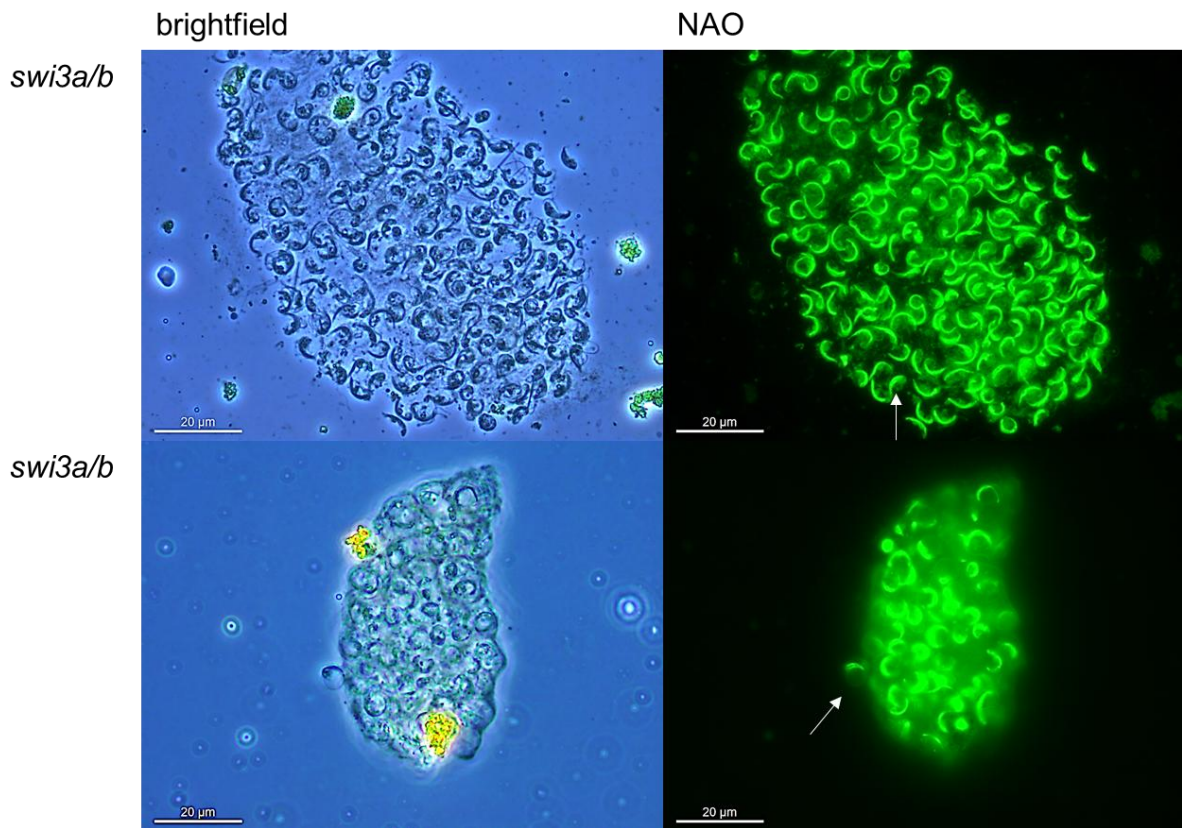


Figure S11: Spermatozoid analysis via staining with NAO.

Ppswi3a/b antheridia release spermatozoa, which however are embedded in a matrix that may form a caviar-like bubbles (in which the condensing nucleus is surrounded by the extraplasmatic matrix in which gametes differentiate, bottom panel), and/or show incomplete cytoplasmic reduction (upper panel) (white arrows).

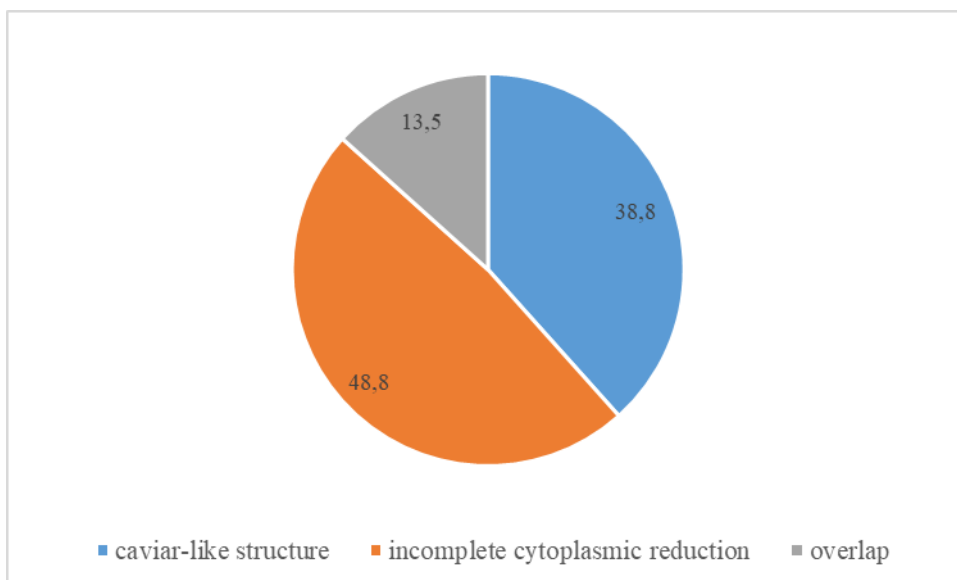


Figure S12: Light microscopical analysis of *Ppswi3a/b* antheridia.

The Caviar-like structure could be seen in 37.8% of the analyzed pictures, whereas the incomplete cytoplasmic reduction was observed in 48.8% of analyzed pictures. An overlap of caviar-like structures and incomplete cytoplasmic reduction was observed in 13.5% of analyzed pictures. 37 pictures were analyzed in total.

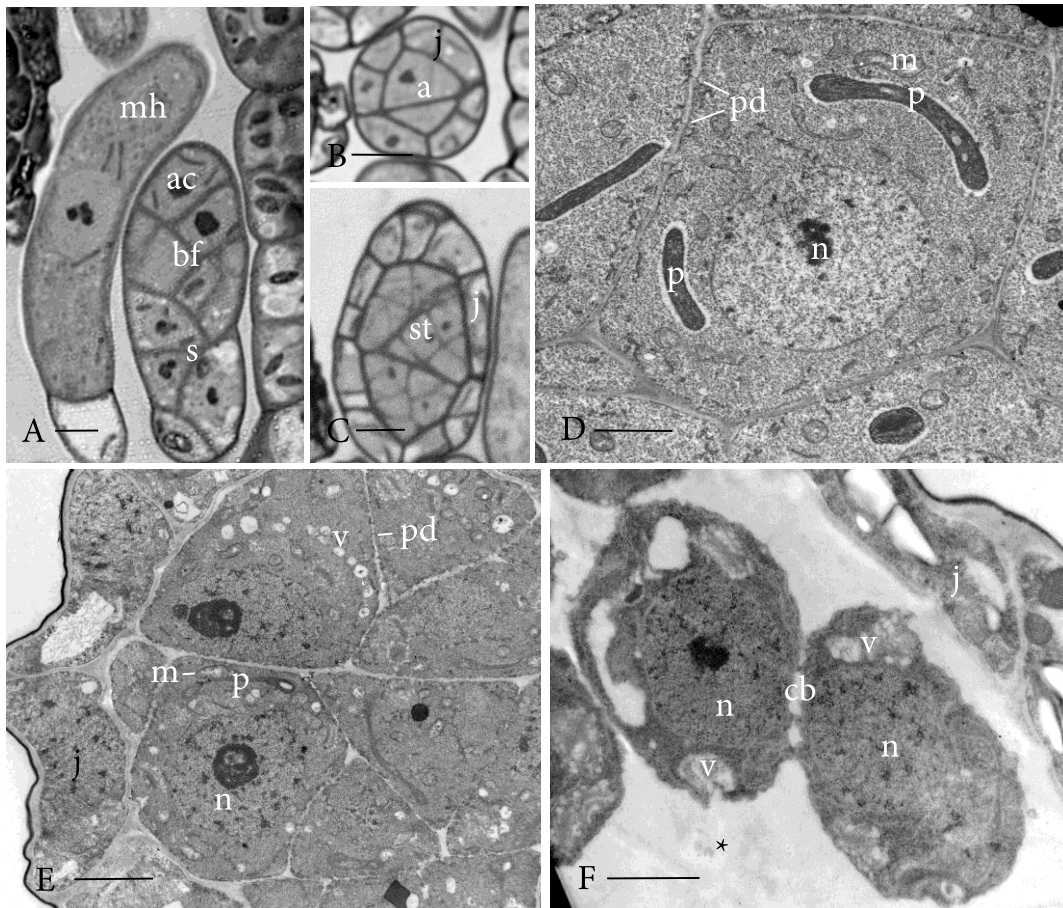


Figure S13: Antheridial develop in Reute and *Ppswi3a/b*

Antheridial development and early spermatids before origin of locomotory apparatus are identical in Reute control and *Ppswi3a/b*. A) Light micrograph (LM) longitudinal section of a developing antheridium with stalk cells (s) showing triangular apical cell (ac) and beginning of biseriate filament (bf) next to a mucilage hair (mh) (Reute). B) LM cross section of the body of an antheridium with two primary androgones (a) surrounded by newly formed jacket cell (j) (*Ppswi3a/b*). C) LM longitudinal section of developing antheridium with spermatogenous tissue (st) surrounded by jacket cells (j) (Reute). D) Transmission electron micrograph (TEM) of dense spermatogenous cell full of ribosomes and endoplasmic reticulum with large nucleus (n), mitochondria (m) and two plastids (p) at the poles preparing for mitosis. Plasmodesmata (pd) are abundant in young walls (Reute). E) TEM of nascent spermatid with large nucleus (n) and dense cytoplasm containing abundant ribosomes, ER, vesicles (v), a single plastid (p) and numerous plasmodesmata (pd), surrounded by jacket cells (j) (*Ppswi3a/b*). F) Young spermatids deposit thick cell wall (*) via vesicles (v) and round out prior to developing the locomotory apparatus. Pairs of spermatids with large nuclei (n) are connected by expanded plasmodesmata that form cytoplasmic bridges (cb). Jacket cells (j) border the antheridium (*Ppswi3a/b*). Bars: A-C = 10 μ m; D-F = 2 μ m.

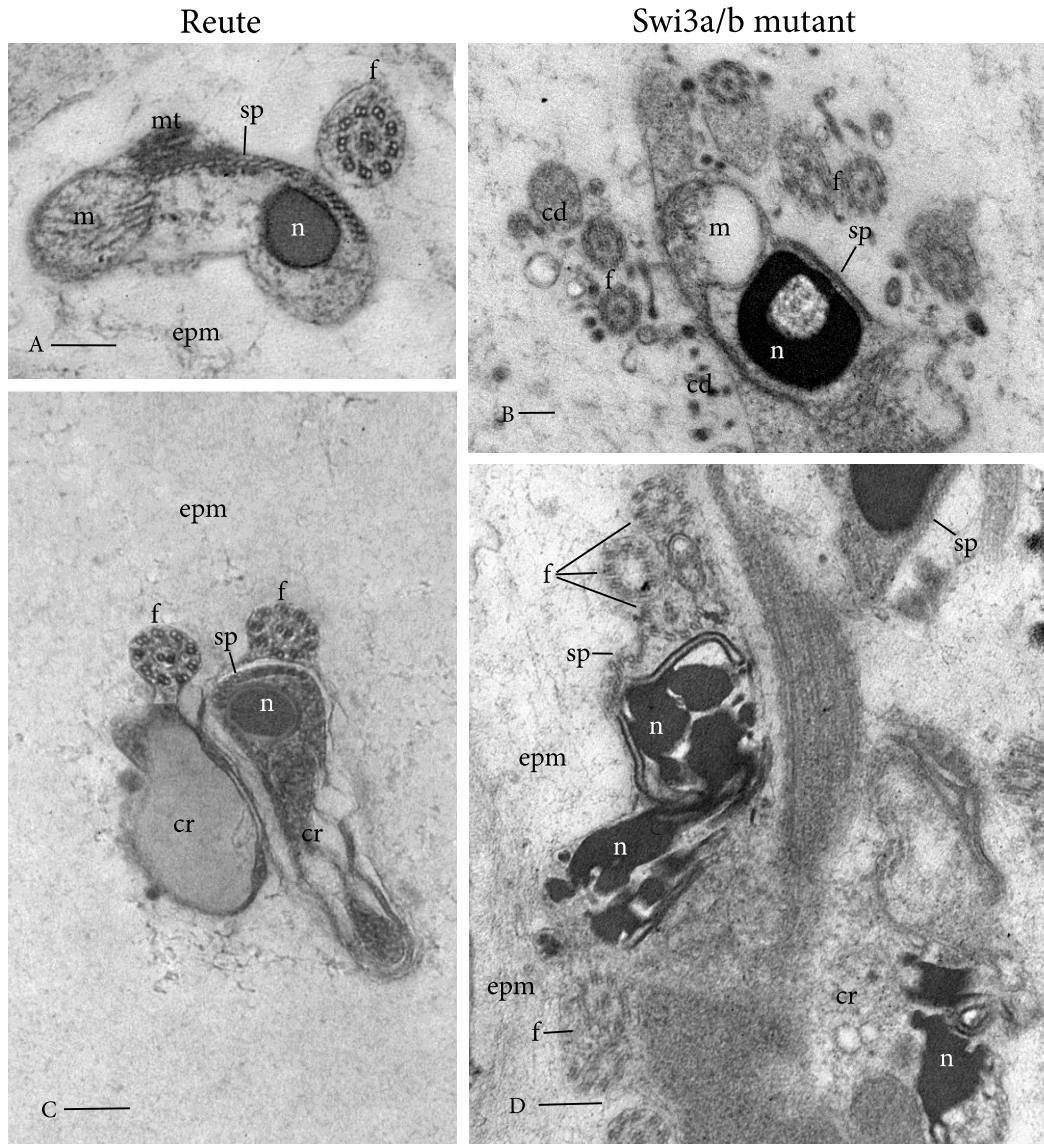


Figure S14: TEM details of mature, unreleased spermatozoids in Reute and Ppswi3a/b

Reute control in left column and Ppswi3a/b mutant in right column. A) Cross section of front of the spermatozoid showing condensed nucleus (n) and mitochondrion (m) under a broad spline (sp) composed of a band of 23 microtubules. The 9+2 flagellum (f) and microtubules (mt) that identify the insertion of the second flagellum are visible. The extraprotoplasmic matrix (epm) is homogeneous with scattered fibrils and devoid of debris. B) Cross section of the spermatozoid more or less comparable to that of A) showing mitochondrion (m) and unevenly condensed nucleus (n) under a spline (sp). Due to the disrupted development in the mutant, the numerous profiles of flagella (f) are haphazardly arranged, and the cytoplasm debris (cd) fills the extraprotoplasmic matrix (epm). C) Cross section of posterior cell profile showing two flagella (f) and a spline (sp) of +/- 12 microtubules over condensed nucleus (n). The homogeneous extraprotoplasmic matrix (epm) is devoid of cytoplasmic debris and the cytoplasmic remnants (cr) are attached to the cell. D) The mutant has multiple disruptions of the flagella (f), nuclear condensation (n), and spline arrangement (sp). The cytoplasm contains massive and irregular cytoplasmic remnants (cr) and the extraprotoplasmic matrix (epm) contains irregular fibrils and cytoplasmic debris. Bars: A-D = 0.2 μ m.

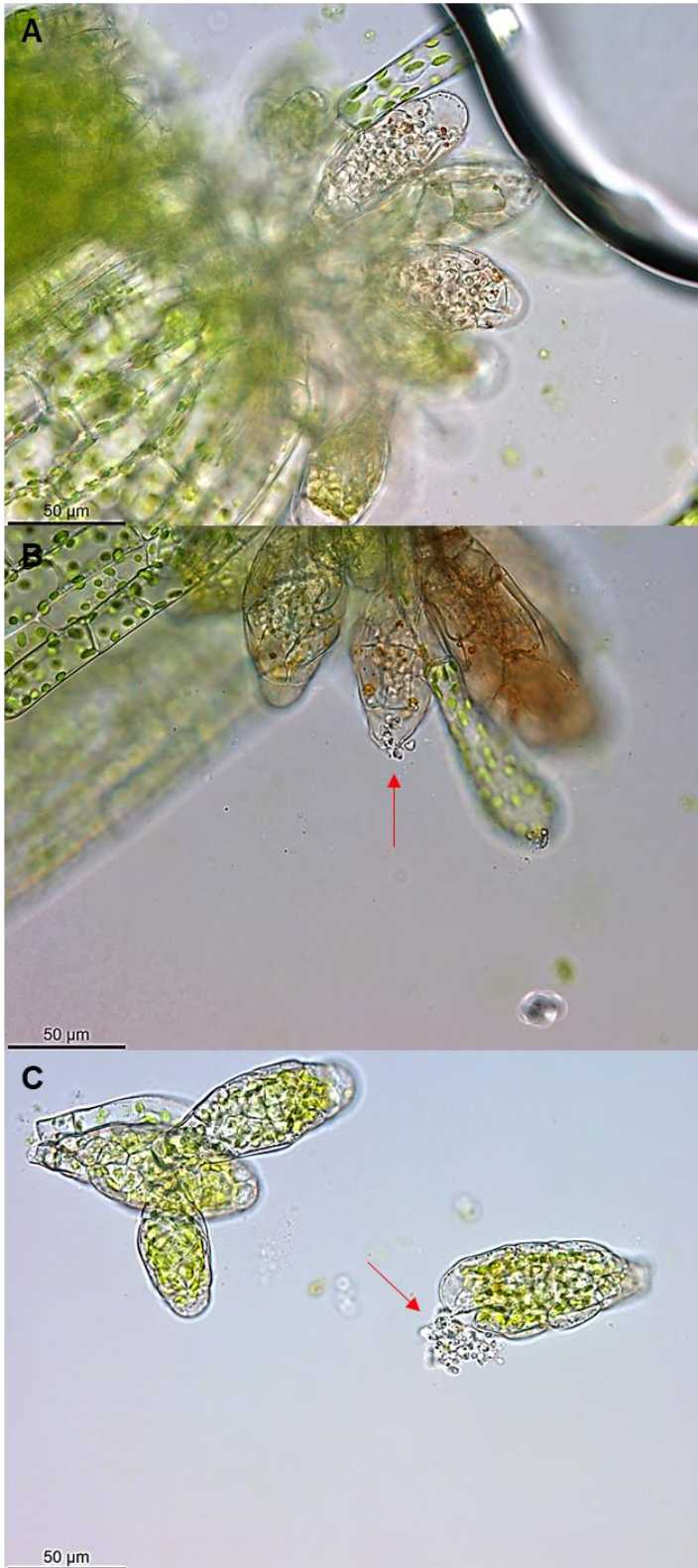


Figure S15: *Pphag1* antheridia development 28 dpi.

A) Closed antheridia turned brownish and discolored. B/C) Opened antheridia released round, bulky spermatozoid agglomerates (indicated by red arrows).

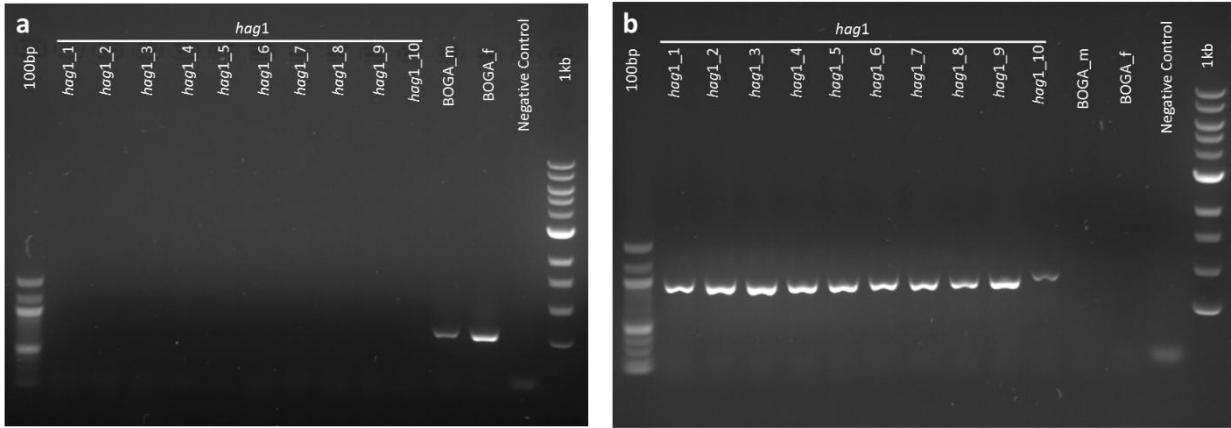


Figure S16: Genotyping of *M. polymorpha* *hag1* mutants.

Presence of the wild type locus was tested using M187s0003_geno_fwd/M187s0003_geno_rev (Table S4). Loss of the wild type locus was verified using M187s0003_geno_fwd/ M187s0003_geno_rev2.

WT

Mphag1

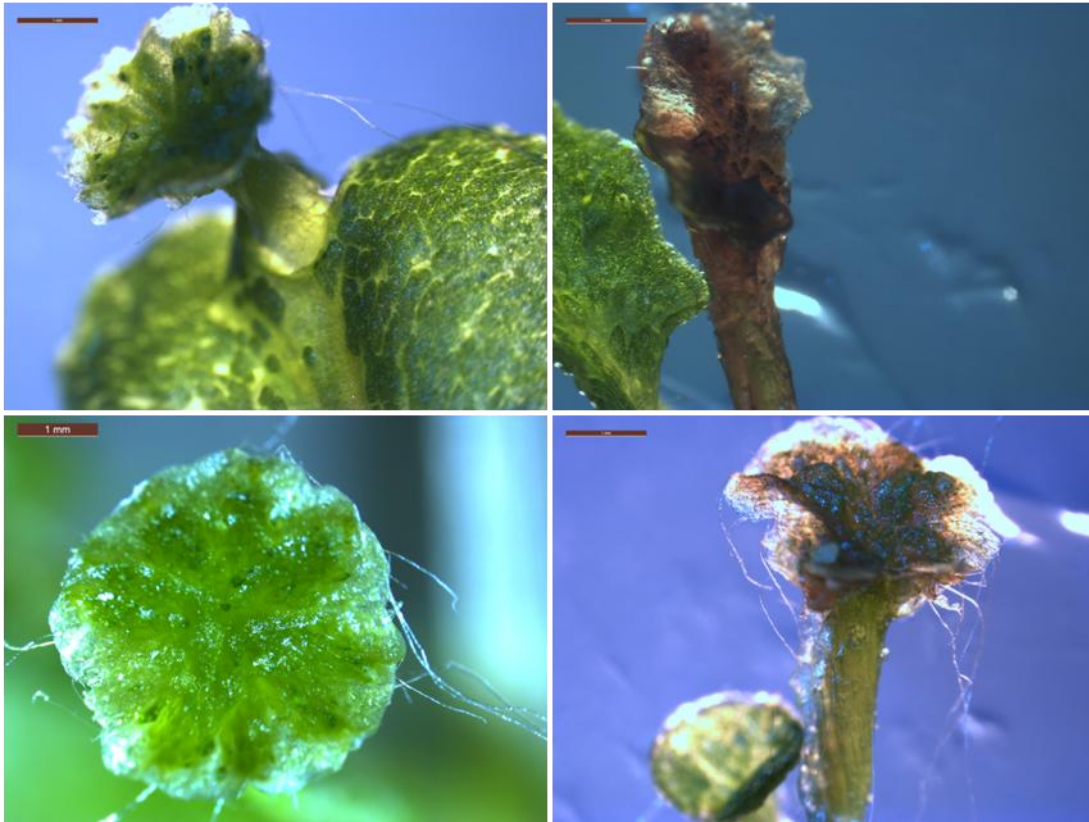


Figure S17: Antheridiophore development of *Mphag1* mutants compared to the control.

Gametangiophores (antheridiophores) developed on top of the thallus after cold and far-red light induction for four weeks. The mutant shows compared to the wild type distorted antheridiophores, occurring before the antheridial receptacle shallowly divided into eight lobes, which has been recognized as a characteristic of antheridial maturity [8].

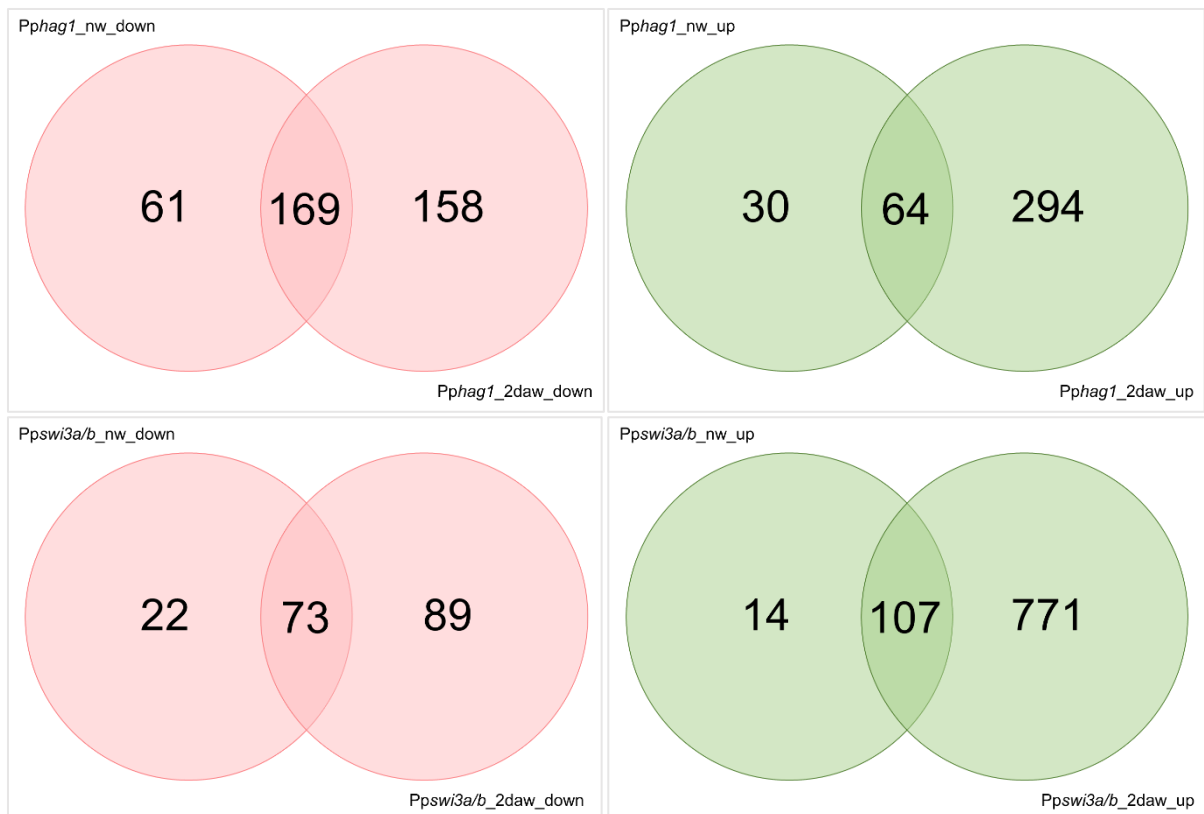


Figure S18: RNA-seq analysis, DEGs.

Number of DEGs 21 dpi of gametangiogenesis induction (nw = not watered), respectively two days after watering (2daw/23dpi). Each Venn diagram compares the DEGs between the two conditions 21 dpi and 2 daw. The color code indicates up-regulated DEGs (green) in the respective mutant (*Pphag1*/*Ppswi3a/b*) compared to the control as well as down-regulated DEGs (red) in the respective mutant (*Pphag1*/*Ppswi3a/b*) compared to the control.

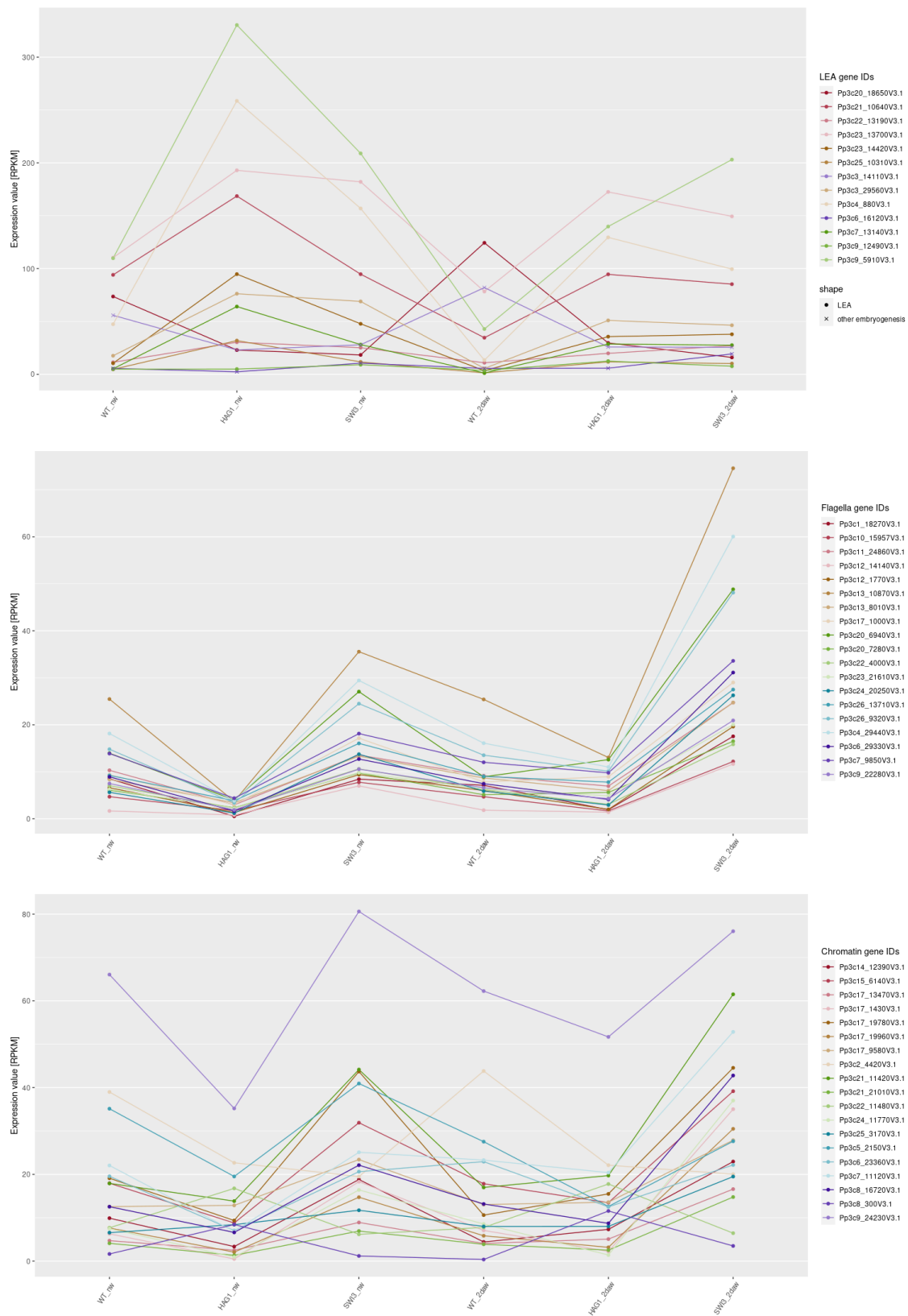


Figure S19: Expression profile of LEA, flagella and chromatin associated DEGs.

Genes carrying annotation terms “embryogenesis”, “flagella” or “chromatin” (Table S7) are shown. The expression [RPKM value] of each experiment is shown as the average of RNA-seq sample triplicates. Over all, the DEGs follow a uniform pattern. Embryogenesis/LEA DEGs show higher expression in the HAG1 mutants while flagella and chromatin related DEGs show higher expression in SWI3 mutants. See Results for details.

Tables

Table S1: Candidate gene selection analysed in terms of single copy status via Bayesian inference.

The number of *P. patens* orthologs is depicted by the arrow colour (green=one, orange=two, red=no). The table lists information of the respective gene, e.g. *P. patens*, *A. thaliana* identifier, TAPscan family, TAIR description/GO biological process [9].

TAP family	<i>P. patens</i> Identifier	Bayesian inference	TAIR10_id	Tair description/GO biological process
C2H2	Pp3c11_480V3.1	(↑) two paralogs	AT1G72050	Encodes a transcriptional factor TFIIIA required for transcription of 5S rRNA gene. 5S rRNA is the smallest constituent of the ribosome. Work on one of the gene models AT1G72050.2 showed that it encodes a protein with nine Cys(2)-His(2)-type zinc fingers, a characteristic feature of TFIIIA proteins. AT1G72050.2 also contains a 23 amino acid spacer between fingers 1 and 2, a 66 amino acid spacer between fingers 4 and 5, and a 50 amino acid non-finger C-terminal tail. in vitro assay demonstrated that AT1g72050.2 binds to 5S rDNA and efficiently stimulates the transcription of 5S rRNA. AT1g72050.2 also binds to 5S rRNA in vitro. AT1g72050.2 is located at several nuclear foci including the nucleolus and is absent from the cytoplasm. multicellular organism development, regulation of transcription, DNA-templated, transcription, DNA-templated
FHA	Pp3c12_14900V3.1	↑	AT5G47790	SMAD/FHA domain-containing protein ; CONTAINS InterPro DOMAIN/s: SMAD/FHA domain (InterPro:IPR008984), Forkhead-associated (FHA) domain (InterPro:IPR000253); BEST Arabidopsis thaliana protein match is: SMAD/FHA domain-containing protein (TAIR:AT5G38840.1)
GNAT	Pp3c5_21790V3.1	↓ no clear ortholog	AT2G39020	ornithine metabolic process; Although this locus shares considerable sequence similarity with the adjacent NATA1 gene (At2g39030), they appear to encode genes with different functions. NATA1 is involved in the production of N-delta-acetylornithine, but, overexpression of At2g39020 in tobacco does not lead to the formation of this defense compound. The mRNA is cell-to-cell mobile.
GNAT	Pp3c7_5970V3.1	(↑) two paralogs	AT5G13780	embryo development ending in seed dormancy, response to water deprivation
GNAT	Pp3c2_9560V3.1	↑	AT3G54610	Encodes a histone acetyltransferase that is plays a role in the determination of the embryonic root-shoot axis. It is also required to regulate the floral meristem activity by modulating the extent of expression of WUS and AG. In other eukaryotes, this protein is recruited to specific promoters by DNA binding transcription factors and is thought to promote transcription by acetylating the N-terminal tail of histone H3. The enzyme has indeed been shown to catalyse primarily the acetylation of H3 histone with only traces of H4 and H2A/B being acetylated. Non-acetylated H3 peptide or an H3 peptide that had been previously acetylated on K9 both serve as excellent substrates for HAG1-catalyzed acetylation. However, prior acetylation of H3 lysine 14 blocks radioactive acetylation of the peptide by HAG1. HAG1 is specific for histone H3 lysine 14. flower development, histone acetylation, positive regulation of transcription, DNA-templated, regulation of vegetative phase change, response to light stimulus, root morphogenesis, transcription, DNA-templated
Jumonji_Other	Pp3c23_15970V3.1	↑	AT5G06550	Encodes a HR demethylase that acts as a positive regulator of seed germination in the PHYB-PIL5-SOM pathway. cell surface receptor signaling pathway, histone H4-R3 methylation, positive regulation of seed germination

Med7	Pp3c5_20850V3.1	(↑) two paralogs	AT5G03500	Mediator complex, subunit Med7; FUNCTIONS IN: RNA polymerase II transcription mediator activity; INVOLVED IN: regulation of transcription from RNA polymerase II promoter; LOCATED IN: mediator complex; CONTAINS InterPro DOMAIN/s: Mediator complex, subunit Med7 (InterPro:IPR009244); BEST Arabidopsis thaliana protein match is: Mediator complex, subunit Med7 (TAIR:AT5G03220.1)
MYB-related	Pp3c2_24980V3.1	↑	AT2G47620	chromatin remodelling, covalent chromatin modification, multicellular organism development, regulation of transcription, DNA-templated, transcription, DNA-templated
MYB-related	Pp3c14_5130V3.1	(↑) two paralogs	AT5G06110	DnaJ domain ;Myb-like DNA-binding domain; FUNCTIONS IN: heat shock protein binding, DNA binding; INVOLVED IN: protein folding; EXPRESSED IN: 23 plant structures; EXPRESSED DURING: 13 growth stages; CONTAINS InterPro DOMAIN/s: Molecular chaperone, heat shock protein, Hsp40, DnaJ (InterPro:IPR015609), Heat shock protein DnaJ, N-terminal (InterPro:IPR001623), Heat shock protein DnaJ, conserved site (InterPro:IPR018253), MYB-like (InterPro:IPR017877), SANT, DNA-binding (InterPro:IPR001005), Myb, DNA-binding (InterPro:IPR014778), Homeodomain-like (InterPro:IPR009057); BEST Arabidopsis thaliana protein match is: DnaJ domain ;Myb-like DNA-binding domain (TAIR:AT3G11450.1) cell division, protein folding
SET/Sigma70-like	Pp3c14_4440V3.1	↑	AT1G64860	DNA-templated transcription, initiation, cellular response to light stimulus, cellular response to redox state, photosystem stoichiometry adjustment, regulation of RNA biosynthetic process, regulation of transcription, DNA-templated
TUB	Pp3c3_17070V3.1	↓ no clear ortholog	AT2G47900	cellular response to osmotic stress, regulation of transcription, DNA-templated, response to fungus, response to hydrogen peroxide, response to salt stress

Table S2: Detailed numbers of crossing analyses with a fluorescent male fertile strain to test for male impairment.

Ppswi3a/b and *Pphag1* were crossed with Re-mcherry according to [10]. Shown is the number of sporophytes per gametophore (s/g) in percentage relative to the total number of gametophores, and the rate of crosses per sporophytes (c/s) in percentage relative to the total number of sporophytes. Most of the sporophytes in the Reute control derive from selfing (homozygous; hence low number of heterozygous sporophytes, c/s). In contrast, almost 100% of mutant sporophytes are heterozygous, indicating a male impairment. The cross with the male fertile strain could largely restore the phenotype in *swi3a/b* (sporophyte/gametophore ratio at least 80%), while *Pphag1* shows a significantly reduced sporophyte ratio as compared to the control. Three independent replicates were performed for the three mutant lines as well as the control. The total number of gametophores analysed was 621 (*swi3a/b*), 770 (*hag1*) and 190 (control).

Mutant/control	replicate 1 (%)	replicate 2 (%)	replicate 3 (%)
swi3a/b_1 s/g	100.00	82.26	98.81
swi3a/b_1 cs	96.05	100.00	98.80
swi3a/b_2 s/g	100.00	79.78	87.04
swi3a/b_2 cs	100.00	97.18	100.00
swi3a/b_3 s/g	97.33	86.59	100.00
swi3a/b_3 cs	100.00	94.37	96.49
hag1_1 s/g	21.21	14.08	4.00
hag1_1 cs	100.00	100.00	100.00
hag1_2 s/g	60.61	32.89	57.14
hag1_2 cs	100.00	96.00	100.00
hag1_3 s/g	28.81	22.09	46.35
hag1_3 cs	82.35	100.00	96.63
Reute s/g	95.45	95.83	100.00
Reute cs	3.17	2.90	3.85

Table S3: see extra file describing the sources of the genome-derived protein sets used.

Table S4: List of PCR primers used in this study.

name	sequence (5' → 3')
Mapoly0187s0003_sg1_rev	AAACAGTGGATTGTGGCTCTACCC
Mapoly0187s0003_sg2_rev	AAACCCGCAAACATGTCCAGCGTC
M13for	GTAAAACGACGGCCAGT
M13rev	GGAAACAGCTATGACCATG
Mapoly0187s0003#1	ACGTACATGAGAGTACGAAAGCA
Mapoly0187s0003#2	ATACTCCTTTGTTCACAGATGC
Mapoly0187s0003#3	TCACGACTGCAGTACGCTC
Mapoly0187s0003_sg1_for	CTCGGGGTAGAGCCACAATCCACT
Mapoly0187s0003_sg2_for	CTCGGACGCTGGACATGTTTGCGG
Marpo_female_fwd	CACCATGGGCCTACTTGTTCAGTCGCTGGTGG
Marpo_female_rev	TCAAAGGCTAGTGTTCATTACTTGGAC
Marpo_male_fwd	GCAGCTGTGTTTTGTGCAGATCGTC
Marpo_male_rev	ATTCTGACCTTACAAGAAATCCTCC
pJet_rev	GCTGAGAATATTGTAGGAGATCTTCTAG
pJet_uni_neu	CAACTGCTTTAACACTTGTGCCTG
Pp3c2_24980#1	TGCTTCCAAGGAGGCGAAAC
Pp3c2_24980#2	ACTATGCAACTCCATCACTCCAGG
Pp3c2_24980#3-EcoR1	GAATTCATGGTGAACCCGGCG
Pp3c2_24980#4-Xba1	TCTAGATGAACTGGGCGCAGGG
Pp3c2_9560#1	TCCAACGGTGATTCTCGCAG
Pp3c2_9560#2	AGGTGCTCCCGAGATACG
Pp3c2_9560#3	TCGTCAGGATCCGTTCCAATG
Pp3c2_9560#4-EcoR1	GAATTCATGCGCAAGGGGGCC
Pp3c2_9560#5-Sal1	GTCGACTGACAAGTGTGTGATCTGCTGACCAAC

Table S5: List of sgRNAs expression cassettes used in this study.

Promoter sequences are in blue, target sequences in red and tracrRNA sequences in green. For *M. polymorpha* tracrRNA and promoter were already implemented in the vectors ordered from Addgene.

Name	Sequence (5'-3')
Pp3c2_9560-sgRNA1	GTCCATTGAAGCAGACGTGTTGCGACAGGTTAGCGACGATGGGTGTAGATGTGATGTGATG TGATGGTGTGGTTCTTCCACGGCGGCGTCTTTCGCGGTGGCGGAGAAGGGGATATCCCGAAG GAGCGGCAGCGGGAGAGCACAAGCAGAAAGGTTGCAGTGAGTGAGTGGGTCCAGCTGGGT GGCTGGCCGAGTGGACGCGACCGGGTTTCGAGGGGGGGGGGAGAAAAGGGATGGAGCG AGGGATATAACCCACATGGAATGGAGGTGGGTGTGAAGGCGGGTATATAGGAAGGTGGAG GACTTACAACCCATgcccacaactttcaacggGTTTTAGAGCTAGAAAATAGCAAGTAAAAATAAGGC TAGTCCGTTATCAACTTGAAAAAGTGGCACCGAGTCCGGTGCTTTTTTT
Pp3c2_9560-sgRNA2	GTCCATTGAAGCAGACGTGTTGCGACAGGTTAGCGACGATGGGTGTAGATGTGATGTGATG TGATGGTGTGGTTCTTCCACGGCGGCGTCTTTCGCGGTGGCGGAGAAGGGGATATCCCGAAG GAGCGGCAGCGGGAGAGCACAAGCAGAAAGGTTGCAGTGAGTGAGTGGGTCCAGCTGGGT GGCTGGCCGAGTGGACGCGACCGGGTTTCGAGGGGGGGGGGAGAAAAGGGATGGAGCG AGGGATATAACCCACATGGAATGGAGGTGGGTGTGAAGGCGGGTATATAGGAAGGTGGAG GACTTACAACCCATggttcgaaggtgcgaacggGTTTTAGAGCTAGAAAATAGCAAGTAAAAATAAGGC TAGTCCGTTATCAACTTGAAAAAGTGGCACCGAGTCCGGTGCTTTTTTT
Pp3c2_24980-sgRNA1	GTCCATTGAAGCAGACGTGTTGCGACAGGTTAGCGACGATGGGTGTAGATGTGATGTGATG TGATGGTGTGGTTCTTCCACGGCGGCGTCTTTCGCGGTGGCGGAGAAGGGGATATCCCGAAG GAGCGGCAGCGGGAGAGCACAAGCAGAAAGGTTGCAGTGAGTGAGTGGGTCCAGCTGGGT GGCTGGCCGAGTGGACGCGACCGGGTTTCGAGGGGGGGGGGAGAAAAGGGATGGAGCG AGGGATATAACCCACATGGAATGGAGGTGGGTGTGAAGGCGGGTATATAGGAAGGTGGAG GACTTACAACCCATgcccggagccactcccgaagGTTTTAGAGCTAGAAAATAGCAAGTAAAAATAAGGC CTAGTCCGTTATCAACTTGAAAAAGTGGCACCGAGTCCGGTGCTTTTTTT
Pp3c2_24980-sgRNA2	GTCCATTGAAGCAGACGTGTTGCGACAGGTTAGCGACGATGGGTGTAGATGTGATGTGATG TGATGGTGTGGTTCTTCCACGGCGGCGTCTTTCGCGGTGGCGGAGAAGGGGATATCCCGAAG GAGCGGCAGCGGGAGAGCACAAGCAGAAAGGTTGCAGTGAGTGAGTGGGTCCAGCTGGGT GGCTGGCCGAGTGGACGCGACCGGGTTTCGAGGGGGGGGGGAGAAAAGGGATGGAGCG AGGGATATAACCCACATGGAATGGAGGTGGGTGTGAAGGCGGGTATATAGGAAGGTGGAG GACTTACAACCCATgcaactccagagctcgcaccGTTTTAGAGCTAGAAAATAGCAAGTAAAAATAAGGC CTAGTCCGTTATCAACTTGAAAAAGTGGCACCGAGTCCGGTGCTTTTTTT
Mapoly0187s0003.1_sgRNA1	CTACTACACTCCTCAACGCAAGTTCTATCTCATATCTCTGCAAGAGCTTATTCCAAGAAACT TTCTTGTGCTTCTATGCATGCCAGGTACCTTAAGTCGCGCGCATAGTCACCTTCACAGCCTTT TCAGTTCTCCCTTTGATGGCTCAGAGTGACGCAACTGCACAAAAATAAGAAAAAAGTCGAA GCGTACGAGAGATGTATCCGGCTAGTTTCTTGGAGTTCGGATTGCTCTCTTTCTCTGTCTC CCCGAACCATATGGAATTTATGAACTGCTGTTCACTAGTCAGTCACTTGTTCAGAACTTTT GAGTGGTCGATTTATCCACCTTCTTGTTCCTGGGTCCAGAATCTGACTTCTTGAGACAA CAAACAGTGCACAGTGGATCGAAGAATGACCACAGTTGAGACACGTGGCGCTGGCCTCATT TATTGCACCATACGTTTGTGAAGAAGTGAATAATGGTGGATATAAAGCAGAGTTGCACCC AGCCTCTggtagagccacaactccactGTTTTAGAGCTAGAAAATAGCAAGTAAAAATAAGGCTAGTCC GTTATCAACTTGAAAAAGTGGCACCGAGTCCGGTGCTTTTTTT
Mapoly0187s0003.1_sgRNA2	CTACTACACTCCTCAACGCAAGTTCTATCTCATATCTCTGCAAGAGCTTATTCCAAGAAACT TTCTTGTGCTTCTATGCATGCCAGGTACCTTAAGTCGCGCGCATAGTCACCTTCACAGCCTTT TCAGTTCTCCCTTTGATGGCTCAGAGTGACGCAACTGCACAAAAATAAGAAAAAAGTCGAA GCGTACGAGAGATGTATCCGGCTAGTTTCTTGGAGTTCGGATTGCTCTCTTTCTCTGTCTC CCCGAACCATATGGAATTTATGAACTGCTGTTCACTAGTCAGTCACTTGTTCAGAACTTTT GAGTGGTCGATTTATCCACCTTCTTGTTCCTGGGTCCAGAATCTGACTTCTTGAGACAA CAAACAGTGCACAGTGGATCGAAGAATGACCACAGTTGAGACACGTGGCGCTGGCCTCATT TATTGCACCATACGTTTGTGAAGAAGTGAATAATGGTGGATATAAAGCAGAGTTGCACCC AGCCTCTgacgctggacatgtttcggGTTTTAGAGCTAGAAAATAGCAAGTAAAAATAAGGCTAGTCCG TTATCAACTTGAAAAAGTGGCACCGAGTCCGGTGCTTTTTTT

Table S6: Detailed numbers of gametangiophore development analyses for *Marchantia polymorpha*.

Three independent replicates (three ECO2 boxes with two plants respectively) were analysed with regard to the mutant lines as well as the wild type (WT; m=male, f=female). The mutant lines were numbered consecutively.

Lines	Replicate 1		Replicate 2		Replicate 3	
	Plant 1	Plant 2	Plant 1	Plant 2	Plant 1	Plant 2
<i>hag1_1</i>	0	0	4	2	0	0
<i>hag1_2</i>	0	0	0	1	0	0
<i>hag1_3</i>	0	1	0	0	0	0
<i>hag1_4</i>	0	0	0	1	0	0
<i>hag1_5</i>	0	0	0	0	0	0
<i>hag1_6</i>	0	0	6	0	12	2
<i>hag1_7</i>	0	0	0	1	0	0
<i>hag1_8</i>	4	3	25	4	0	0
<i>hag1_9</i>	2	1	0	1	0	1
<i>hag1_10</i>	0	0	1	0	0	0
WT_m	32	32	20	21	49	40
WT_f	40	38	38	50	43	34

Table S7: DEGs annotated as related to embryogenesis (blue; yellow: LEA), chromatin (orange) and flagella (green).

gene_id_v3.3	GO_annot_BP	GO_annot_MF	TAIR_desc	Unigene reviewed_desc	Unigene gene annotation	cosmos_genomaut_description	cosmos_genomaut_annot
Pp3c1_15270v3.1						PREDICTED: ciliated domain-containing protein 147 [Ciona intestinalis]	
Pp3c11_15957v3.1						PREDICTED: cilia- and flagella-associated protein 57-like isoform X1 [Aplysia californica]	
Pp3c11_24860v3.1	protein phosphorylation	protein kinase superfamily protein	MAPK/MAKMKRK overtopping k	PREDICTED: MAPK/MAKMKRK overtopping k		long flagella protein 16	long flagella protein 16
Pp3c12_14140v3.1	anatomical structure morphogenesis	cell projection organization	single-organism development	intraflagellar transport protein 81	PREDICTED: intraflagellar transport protein 81	estrogen-related receptor beta like 1	estrogen-related receptor beta like 1
Pp3c12_1770v3.1						EF-hand domain-containing protein	EF-hand domain-containing protein
Pp3c13_10870v3.1						13 kDa desflagellin-inducible protein	13 kDa desflagellin-inducible protein
Pp3c13_8010v3.1						radial spoke protein 3	radial spoke protein 3
Pp3c14_12390v3.1	hichome morphogenesis	anther	sequence-specific DNA binding	sequence-specific DNA binding transcription factor activity	chiron	transcription repressor MYB4 [Vitis v. MDA7.17; myb family transcription factor]	MDA7.17; myb family transcription factor
Pp3c15_8140v3.1	metabolic process	helicase activity	DNA binding	A	Encodes a SWISWIF nuclease	PREDICTED: chromodomain-helicase-chromodomain-helicase-dna-binding protein:SNF2 family chromodomain-helicase-chromodomain-helicase-dna-binding protein	chromodomain-helicase-dna-binding protein
Pp3c17_1000v3.1						hypothetical protein AMTR_s0000900107000 [Amborella trichopoda]	
Pp3c17_13470v3.1						hypothetical protein M569_04726 [G] hydroxyproline-rich glycoprotein family protein	hydroxyproline-rich glycoprotein family protein
Pp3c17_1430v3.1						PREDICTED: uncharacterized protein F14C21.44; late embryogenesis abundant protein-related / LEA protein-related	F14C21.44; late embryogenesis abundant protein-related / LEA protein-related
Pp3c17_10780v3.1	hichome morphogenesis	anther	sequence-specific DNA binding	sequence-specific DNA binding transcription factor activity	chlor	PREDICTED: myb-related protein 31 MDA7.17; myb family transcription factor	MDA7.17; myb family transcription factor
Pp3c17_19960v3.1						hypothetical protein SELMODRAFT_dynamin like protein	dynamin like protein
Pp3c17_9850v3.1	nucleolus organization	methyl GTP binding	GTPase activity			PREDICTED: uncharacterized protein F14C21.44; late embryogenesis abundant protein-related / LEA protein-related	F14C21.44; late embryogenesis abundant protein-related / LEA protein-related
Pp3c2_4400v3.1						hypothetical protein H57_07862 [Ac] repeat domain 65	
Pp3c20_18650v3.1						PREDICTED: uncharacterized protein F14C21.44; late embryogenesis abundant protein-related / LEA protein-related	F14C21.44; late embryogenesis abundant protein-related / LEA protein-related
Pp3c20_8940v3.1						hypothetical protein H57_07862 [Ac] repeat domain 65	
Pp3c20_7290v3.1						PREDICTED: uncharacterized protein F14C21.44; late embryogenesis abundant protein-related / LEA protein-related	F14C21.44; late embryogenesis abundant protein-related / LEA protein-related
Pp3c21_10640v3.1						late embryogenesis abundant hydroxyproline-rich glycoprotein [Medicago truncatula]	late embryogenesis abundant hydroxyproline-rich glycoprotein [Medicago truncatula]
Pp3c21_11420v3.1	anatomical structure morphogenesis	flower development	single-organism cellular process	cellul	Actin-related protein 4	PREDICTED: actin-related protein 7 actin	actin
Pp3c21_21010v3.1						PREDICTED: uncharacterized protein F14C21.44; late embryogenesis abundant protein-related / LEA protein-related	F14C21.44; late embryogenesis abundant protein-related / LEA protein-related
Pp3c22_11480v3.1	multidimensional cell growth	trich	actin binding	Encodes a WD40 repeat cell	Probable histone-binding protein	WD repeat 2 [Vitis vinifera]	F13823.16; flower pigmentation protein (AN11) [Arabidopsis thaliana]
Pp3c22_13190v3.1	response to desiccation					PREDICTED: actin-related protein 3; actin-like protein	actin-like protein
Pp3c22_4000v3.1						late embryogenesis abundant protein; putative / LEA protein	late embryogenesis abundant protein
Pp3c23_13700v3.1						late embryogenesis abundant protein; putative / LEA protein	late embryogenesis abundant protein
Pp3c23_14420v3.1						protein belonging to late embryogenesis abundant (LEA) protein in group 3 that might be involved in maturation and desiccation tolerance of seeds. RFLP and CAPS mapping place it on chromosome 4 but the nucleotide sequence is identical to that of a protein in group 4	protein belonging to late embryogenesis abundant (LEA) protein in group 3 that might be involved in maturation and desiccation tolerance of seeds. RFLP and CAPS mapping place it on chromosome 4 but the nucleotide sequence is identical to that of a protein in group 4
Pp3c23_21810v3.1						Desflagellin-inducible protein 13 kDa	Desflagellin-inducible protein 13 kDa
Pp3c24_11770v3.1	protein folding	response to heat	DNA binding	chromatin binding	Member of the R2R3 factor gene	Transcription factor MYB57	PREDICTED: myb-related protein M1_r2r3-myb transcription
Pp3c24_20250v3.1						hypothetical protein SELMODRAFT_dynamin like protein	dynamin like protein
Pp3c25_10310v3.1						hypothetical protein SELMODRAFT_dynamin like protein	dynamin like protein
Pp3c25_3170v3.1						hypothetical protein SELMODRAFT_dynamin like protein	dynamin like protein
Pp3c26_13710v3.1	CTP biosynthetic process	nucleoside diphosphate kinase activity	ATP binding			Nucleoside diphosphate kinase	Nucleoside diphosphate kinase
Pp3c26_3020v3.1	single-organism cellular process					intraflagellar transport protein 81	intraflagellar transport protein 81
Pp3c3_14110v3.1	protein phosphorylation	ATP binding	protein serine/threonine	NSP-interacting kinase 2 [NIK2]	Protein NSP-interacting kinase 2 [NIK2]	PREDICTED: somatic embryogenesis	brassinosteroid insensitive 1-associated receptor kinase 1
Pp3c3_26500v3.1						hypothetical protein, variant [Sagittaria dictyna V.S20]	
Pp3c4_29400v3.1						hypothetical protein CAP2/DRAFT_170918 [Capitata telea]	
Pp3c4_880v3.1						late embryogenesis abundant protein; late embryogenesis abundant protein; late embryogenesis abundant protein, group 3 (LEA) (PMA2005) [Triticum aestivum]	late embryogenesis abundant protein; late embryogenesis abundant protein; late embryogenesis abundant protein, group 3 (LEA) (PMA2005) [Triticum aestivum]
Pp3c5_2150v3.1						putative R2R3 MYB protein 5 [Arachis hypogaea transcription factor-like protein]	myb transcription factor-like protein
Pp3c8_18120v3.1	AMP salvage	AMP deaminase activity		Encodes a protein with 7n viral	AMP deaminase	putative R2R3 MYB protein 5 [Arachis hypogaea transcription factor-like protein]	myb transcription factor-like protein
Pp3c8_23360v3.1						PREDICTED: AMP deaminase-like [Cicer arietinum]	
Pp3c8_2630v3.1						Uncharacterized protein C4or2	Uncharacterized protein C4or2
Pp3c7_11120v3.1						PREDICTED: protein REVEILLE 7 [Elymus domain-containing protein]	
Pp3c7_13140v3.1						PREDICTED: protein REVEILLE 7 [Elymus domain-containing protein]	
Pp3c7_13420v3.1	single-organism cellular process	tubulin N-acetyltransferase activity				hypothetical protein SELMODRAFT_64748, partial [Salicornia mollendorffii]	
Pp3c7_7130v3.1	positive regulation of cell motility	sequence-specific DNA binding	transcription factor activity			Alpha-tubulin N-acetyltransferase [microtubule] [Dytricha triflorae]	
Pp3c8_10720v3.1	intracellular transport					UF3468 protein [Phytophthora parasitica INRA-319]	
Pp3c8_300v3.1	protein folding	response to heat	DNA binding	chromatin binding	heat shock protein binding	ATP binding/unfolded protein binding	OS.NB3a0069H10.16 [Oryza sativa japonica Group]
Pp3c9_12490v3.1						late embryogenesis abundant (LEA) hydroxyproline-rich glycoprotein [Glycine max.]	late embryogenesis abundant (LEA) hydroxyproline-rich glycoprotein [Glycine max.]
Pp3c9_2280v3.1						Encodes a putative TATA bind; Spem-associated antigen 16 [p]	PREDICTED: spermiin-associated anti-Flagellar and repeat protein p20
Pp3c9_24230v3.1	sugar mediated signaling pathw	structural constituent of cytosk		Encodes a gene similar to actin	Actin-related protein 4	PREDICTED: actin-related protein 4; actin related protein	actin related protein
Pp3c9_5810v3.1						MUL TSP/ECES: hypothetical protein [Haemophilus]	
Pp3c9_8530v3.1						late embryogenesis abundant protein	late embryogenesis abundant protein
Pp3c9_30v3.1						hypothetical protein SELMODRAFT_F14C21.44; late embryogenesis abundant protein-related / LEA protein-related F14C21.44; late embryogenesis abundant protein-related / LEA protein-related	F14C21.44; late embryogenesis abundant protein-related / LEA protein-related F14C21.44; late embryogenesis abundant protein-related / LEA protein-related

References

1. Lechner M, Findeiss S, Steiner L, Marz M, Stadler PF, Prohaska SJ: **Proteinortho: detection of (co-)orthologs in large-scale analysis.** *BMC Bioinformatics* 2011, **12**:124.
2. Wilhelmsson PKI, Muhlich C, Ullrich KK, Rensing SA: **Comprehensive Genome-Wide Classification Reveals That Many Plant-Specific Transcription Factors Evolved in Streptophyte Algae.** *Genome Biol Evol* 2017, **9**(12):3384-3397.
3. Frickenhaus S, Beszteri B: **Quicktree-SD, Software developed by AWI-Bioinformatics.** In.; 2008.
4. Fernandez-Pozo N, Haas FB, Meyberg R, Ullrich KK, Hiss M, Perroud PF, Hanke S, Kratz V, Powell AF, Vesty EF *et al*: **PEATmoss (Physcomitrella Expression Atlas Tool): a unified gene expression atlas for the model plant Physcomitrella patens.** *Plant J* 2019.
5. Meyberg R, Perroud PF, Haas FB, Schneider L, Heimerl T, Renzaglia KS, Rensing SA: **Characterization of evolutionarily conserved key players affecting eukaryotic flagellar motility and fertility using a moss model.** *New Phytol* 2020.
6. Ortiz-Ramirez C, Hernandez-Coronado M, Thamm A, Catarino B, Wang M, Dolan L, Feijo JA, Becker JD: **A transcriptome atlas of Physcomitrella patens provides insights into the evolution and development of land plants.** *Mol Plant* 2015, **9**:205-220.
7. Perroud PF, Haas FB, Hiss M, Ullrich KK, Alboresi A, Amirebrahimi M, Barry K, Bassi R, Bonhomme S, Chen H *et al*: **The Physcomitrella patens gene atlas project: large-scale RNA-seq based expression data.** *Plant J* 2018, **95**(1):168-182.
8. Shimamura M: **Marchantia polymorpha : Taxonomy, Phylogeny and Morphology of a Model System.** *Plant and Cell Physiology* 2015, **57**(2):230-256.
9. Lang D, Ullrich KK, Murat F, Fuchs J, Jenkins J, Haas FB, Piednoel M, Gundlach H, Van Bel M, Meyberg R *et al*: **The Physcomitrella patens chromosome-scale assembly reveals moss genome structure and evolution.** *Plant J* 2018, **93**(3):515-533.
10. Perroud PF, Meyberg R, Rensing SA: **Physcomitrella patens Reute mCherry as a tool for efficient crossing within and between ecotypes.** *Plant Biol (Stuttg)* 2019, **21 Suppl 1**:143-149.